

See discussions, stats, and author profiles for this publication at: <https://www.researchgate.net/publication/231711598>

Ionic Aggregates in Partially Zn-Neutralized Poly(ethylene-ran-methacrylic acid) Ionomers: Shape, Size, and Size Distribution

ARTICLE *in* MACROMOLECULES · DECEMBER 1999

Impact Factor: 5.8 · DOI: 10.1021/ma991374j

CITATIONS

47

READS

23

3 AUTHORS, INCLUDING:



[Karen I Winey](#)

University of Pennsylvania

331 PUBLICATIONS 11,130 CITATIONS

SEE PROFILE

Ionic Aggregates in Partially Zn-Neutralized Poly(ethylene-*ran*-methacrylic acid) Ionomers: Shape, Size, and Size Distribution

Karen I. Winey,* Jonathan H. Laurer,[†] and Brian P. Kirkmeyer

Department of Materials Science and Engineering, University of Pennsylvania, Philadelphia, Pennsylvania 19104-6272

Received August 12, 1999

ABSTRACT: The ionic aggregates in a series of partially Zn-neutralized poly(ethylene-*ran*-methacrylic acid) ionomers have been imaged using scanning transmission electron microscopy. The profound advantage of this technique is the direct interpretation of the images for the shape, size, and size distribution of the ionic aggregates. Using tilt series and aspect ratios, the aggregates at all neutralization levels (17–78%) and both as-extruded and recrystallized were found to be spherical. The diameter of the Zn-rich aggregates is ~ 2.1 nm and is independent of the neutralization level. The size of the aggregates increased slightly upon recrystallization, and this was more pronounced at higher neutralization levels. The size distribution was described by a size dispersity index and was found to be nearly monodisperse. Finally, at 17% neutralization the ionic aggregates are widely separated relative to the polymer chains. These combined results suggest that the ionic aggregates include segments from the nonionic polymer backbone and that the aggregate morphology is primarily the result of ionic interactions in the system.

Introduction

Semicrystalline ionomers are industrially important materials in adhesives, packaging, engineering thermoplastics, coatings, and more. The most common of these are based on poly(ethylene-*ran*-methacrylic acid), E/MAA, random copolymers partially neutralized with various cations and produced by DuPont under the trade name Surlyn. In 1990, Register and Cooper described the morphology of semicrystalline ionomers as follows: crystalline lamellae separated by an amorphous polymeric matrix that contains isolated cation-rich domains.¹ Their anomalous small-angle X-ray scattering experiments are consistent with the relative electron densities associated with this “three-phase” morphological model. Despite this agreement and the commercial importance of semicrystalline ionomers, a number of fundamental issues have remained unresolved regarding both their morphology and viscoelastic properties. Recently, a number of advanced characterization tools have been applied to these materials with considerable success.

Quiram et al. used time-resolved simultaneous small- and wide-angle X-ray scattering to study the morphology of Na-neutralized E/MAA as a function of thermal treatment.² As is typical of semicrystalline ionomers, the SAXS data contain two maxima which are assigned to the interlamellae spacing and the ionic aggregates. The peak maxima were detected during isothermal recrystallizations without separating the overlapping lamellae and ionomer peaks as briefly described by Verma et al.³ Among their findings is a shift in the ionomer peak to lower scattering angles as the ionomer melts and a smaller shift to higher scattering angles upon isothermal recrystallization. (The presence of an ionomer peak in the melt is consistent with the considerable thermal stability of the ionic aggregates.⁴) For

example, during an isothermal recrystallization at 64 °C of partially Na-neutralized E/MAA, the ionomer peak maximum increased from 1.6 nm^{-1} in the melt to 2.15 nm^{-1} which apparently indicates a considerable reduction in the size of the ionic aggregates. Furthermore, an analysis of the integrated intensity of the ionomer peak suggests that the electron density of the aggregates decreases and/or the concentration of ionic aggregates in the amorphous phase increases. Given the uncertainty and complexity of SAXS models for ionomers, the authors did not determine the shape, size, or size distribution of the ionic aggregates.

Grady et al. employed extended X-ray absorption fine structure (EXAFS) to determine the local structure about the Zn cations in partially neutralized E/MAA ionomers.⁵ Four oxygen atoms were found to surround the Zn atoms with distances of ~ 0.196 nm. This local environment is consistent with the crystal structure of monoclinic anhydrous zinc acetate. These findings were independent of the neutralizing agent, neutralizing method, level of MAA in the copolymer, and the extent of neutralization (25%–100%). In a separate study, partially Zn-neutralized E/MAA ionomers were immersed in water for a few days until the weight was constant.⁶ EXAFS spectra were virtually unchanged by the water absorption in this system, which indicates only slight changes in the local Zn environment. Thus, the authors conclude that water absorbs only to the edges of their proposed planar ionic aggregates.

Scattering and spectroscopy methods probe volumes on the order of $\sim 0.5 \text{ nm}^3$ and rely on morphological models to interpret the data. In the field of ionomers, detailed analyses of scattering and spectroscopic data are limited due to the absence of verified, quantitative morphological models. In particular, the shape, size, size distribution, and spatial distribution of the ionic aggregates in ionomers remain to be determined via a model-independent method. This is the focus of our research effort in ionomers. Our preliminary results suggest that the ionic aggregates can change dramati-

* To whom correspondence should be addressed.

[†] Current address: Lexmark International, Inc., Lexington, KY 40550.

cally with the anion type and/or preparation methods.⁷

Recently, Laurer and Winey imaged the ionic aggregates using a scanning transmission electron microscope equipped with a field emission electron gun.⁸ This microscopy method offers the advantages of reduced phase contrast, high spatial resolution, and enhanced atomic number contrast relative to transmission electron microscopy. In addition, sample preparation involved only cryo-ultramicrotomy, so that the observed structures are indicative of the bulk morphology. Our initial paper demonstrated the applicability of this technique by showing contrast reversal in a bright field/dark field image pair in a commercial-grade E/MAA ionomer partially neutralized with Zn.

A number of experimental improvements were implemented for the current study. Here, the materials were prepared from the same E/MAA copolymer to eliminate variations in the molecular architecture and copolymer composition. Image quality and resolution have been improved, and a more rigorous feature analysis protocol was developed to evaluate aggregate shape, size, and size distribution. Model-independent data on the morphology of ionic aggregates are critical to understanding the nature of the ionic interactions in ionomers.

Experimental Methods

Materials and Sample Preparation. The materials for this study were prepared using typical commercial methods and provided by Dr. John Paul of DuPont. A single poly(ethylene-*ran*-methacrylic acid) random copolymer was used that has 11 wt % (~4 mol %) of the methacrylic acid units. Using ZnO in a melt extrusion process, this copolymer was neutralized to the following extents: 17, 29, 55, 68, and 78 mol %. We designate the 17% neutralized copolymer as Zn17 and likewise for the other neutralization levels. These same partially neutralized materials have been studied by B. P. Grady via EXAFS.⁶ These extruded pellets were either used as-received or annealed at 115 °C for 1–10 days under vacuum followed by slowly cooling to room temperature. Both “as-extruded” and “recrystallized” samples were microtomed using a Reichert-Jung Ultracut S at –100 °C using a diamond knife. Sections of 50 nm nominal thickness were collected on standard electron microscopy grids. This solvent-free, cryo-method of making sections was designed to maintain the bulk morphology of the ionomers.

Scanning Transmission Electron Microscopy. Scanning transmission electron microscopy (STEM) was performed on a JEOL 2010F analytical electron microscope equipped with a Gatan image filter (GIF). The STEM detectors of the GIF were used to collect annular dark field (ADF) images. Typical imaging conditions are as follows: 197 kV, 1 nm probe size, 50 μ m condenser aperture, 10 cm camera length, and 800 000 magnification. Images (512 \times 408 pixels) require 21 s to collect, so that at these imaging conditions the dose to the specimen is $\sim 6 \times 10^6$ e[–]/nm². Beam damage was determined to be insignificant in these samples, because multiple images from the same sample region are indistinguishable. The typical combination of magnification and image size corresponds to a spatial resolution of 0.28 nm per pixel.

Image Analysis. Standard image analysis methods were used to determine the size and aspect ratio of the features using IMIX software from Princeton Gamma-Tech. The first step was to convert a gray scale image to a binary image in order to identify the Zn-rich ionic aggregates. This is accomplished by setting a threshold gray level, so that pixels with lower or higher gray levels in the ADF-STEM images are assigned to the matrix or aggregates, respectively. The threshold was selected separately for each image by visually comparing the original gray scale image and the corresponding binary image. The features, that is adjacent “aggregate” pixels, were then characterized. The diameter of a feature is calculated as the average of 12 chords across the feature evenly

spaced at 30° increments. The aspect ratio of a feature is the maximum chord divided by the chord which is perpendicular to the maximum chord. For samples of 29% neutralization or higher, 300–600 features were detected and characterized per image.

Setting the threshold does influence the measured values of diameter but does not significantly affect the aspect ratio. For example, a binary image constructed using the optimum threshold has features with an average diameter of 1.74 nm and an aspect ratio of 1.46 for the as-extruded Zn78 sample. If the threshold is set lower by 10 gray levels for the same image, some of the adjacent features in the image are combined into single features, and the average feature diameter increases to 2.09 nm while the aspect ratio is virtually unchanged at 1.47. Conversely, if the threshold is set at 10 gray levels above the optimum threshold for this image, the average feature diameter decreases to 1.49 nm and the aspect ratio is 1.42. Thus, our certainty in the average feature diameter as a function of threshold criteria corresponds approximately to ± 1 pixel, 0.28 nm. This corresponds to $\sim 15\%$ of the average feature size.

Results

As-Extruded Materials. The as-extruded materials exhibit Zn-rich aggregates that appear bright in annular dark field STEM images (Figure 1). This conclusion is based on the fact that the intensity in ADF-STEM increases with atomic number. Specifically, the scattering cross section for Rutherford events increases as Z^2 , where Z designates the atomic number.⁹ The Zn-rich aggregates are present at all the neutralization levels evaluated, 17–78%. In addition, there is a dramatic increase in the areal number density of aggregates between 17% and 29% neutralization. Note that for randomly distributed aggregates the areal number density of aggregates in a STEM image increases linearly with microtomed section thickness. Variations in section thickness do occur during microtomy but are limited to a factor of <2 . Thus, the increase in areal number density between 17% and 29% neutralization from ~ 700 to ~ 9000 aggregates/ μ m² is significant and corresponds to an increase in the volume fraction of aggregates. The apparent volume fraction of aggregates is approximately constant as the neutralization level is further increased.

The shape of the ionic aggregates was determined using both a tilt series and the measured aspect ratios. Figure 2 shows a tilt series of Zn17 in which the same region is viewed from two directions. As expected when rotating about the y -axis, the positions along the y -axis are fixed, while the relative positions along the x -axis change with the tilt angle. Several aggregates are marked to illustrate this point, and the aspect ratios of these isolated aggregates are given in Table 1. As discussed above, the diameter of a feature is known to within 1 pixel (0.28 nm), and given this uncertainty aspect ratios ≤ 1.35 can correspond to individual, circular features. Thus, the features in Zn17 correspond to spherical aggregates, because (1) all the aspect ratios are consistent with circular projections and (2) the aspect ratios for individual aggregates do not change as the specimen is tilted. An isotropic distribution of disklike aggregates in which the diameter is ~ 10 times the thickness would result in features having a wider range of aspect ratios. Thus, we conclude that the Zn-rich ionic aggregates in Zn17 are spherical.

Tilt series at higher levels of neutralization were not interpretable due to the high number density of aggregates in the images. This high number density also causes overlap between the projections of individual

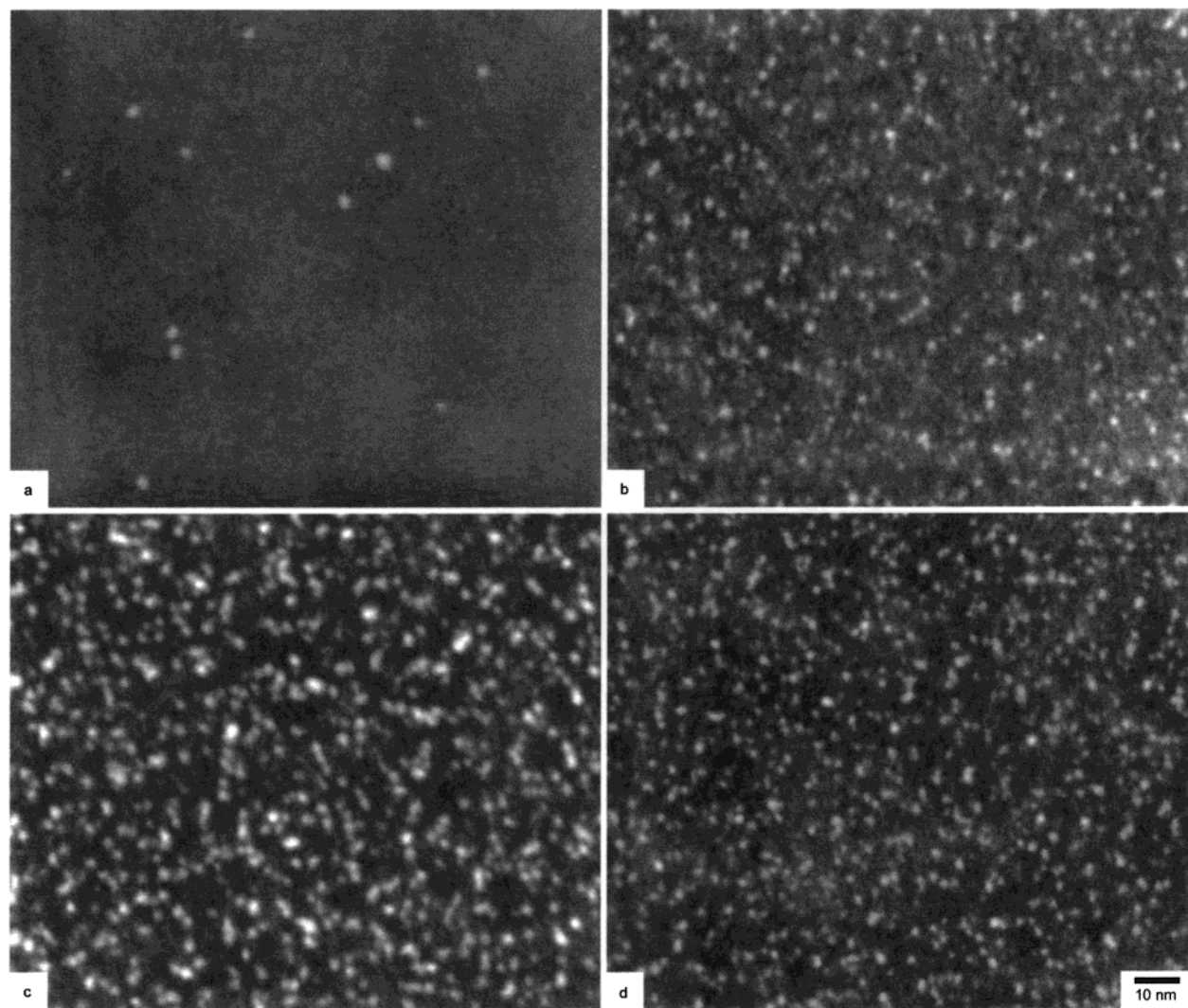


Figure 1. Annular dark field scanning transmission electron microscopy (ADF-STEM) images of as-extruded poly(ethylene-*ran*-methacrylic acid) random copolymer neutralized to various extents with Zn^{2+} : (a) 17%, (b) 29%, (c) 55%, (d) 78%. Bright regions correspond to higher average atomic number. Nearly spherical ionic aggregates of ~ 2.1 nm are present at all neutralization levels, though the areal number density of aggregates increases substantially between 17% and 29% neutralization.

aggregates which artificially increases the aspect ratio. Typical image analysis methods to separate overlapping features were unsuitable for these images. The mean aspect ratios calculated from 300 to 600 features for the as-extruded samples are 1.49, 1.38, 1.52, and 1.41 for Zn29, Zn55, Zn68, and Zn78, respectively. Taking into account the uncertainties of the diameter and aggregate overlap, we conclude that the Zn-rich ionic aggregates at these higher neutralization levels are nearly spherical.

The size of the nearly spherical ionic aggregates was characterized by the diameters of the features. Each specimen exhibits a distribution of feature diameters, so the mean diameter and the size dispersity index are used to describe the aggregate size in each specimen (Figure 3). Note that the error bars in Figure 3a correspond to ± 1 pixel or ± 0.28 nm. The size dispersity index is the ratio of the second and first moments of the diameter, where unity corresponds to a monodisperse system. The as-extruded samples exhibit a range in size dispersity index from 1.06 to 1.27 that is independent of the level of neutralization. Given the presence of overlap and the certainty in the measurement of the diameter, we conclude that these Zn-rich ionic aggregates are nearly monodisperse in diameter.

Furthermore, as a function of the neutralization level, the mean diameter of the aggregates is constant at ~ 2.1 nm within the error of 1 pixel.

The same diameter and size dispersity index values were measured from bright field and annular dark field STEM images. Furthermore, images were collected at higher magnifications ($1\,500\,000\times$) for selected samples, and the mean diameter and size dispersity index were unchanged. These results provide additional confidence in our description of the ionic aggregates as nearly spherical, monodisperse features of diameter ~ 2.1 nm.

Recrystallized Materials. The ionic aggregates were also examined after the extruded pellets were annealed quiescently at 115°C and slowly cooled to room temperature. This heat treatment is in contrast to the rapid quench used in the melt extrusion method. Figure 4 shows ADF-STEM images of Zn29 and Zn78 after a 72 h anneal that are comparable to Figure 1. The mean aspect ratios are 1.35 and 1.51 for Zn29 and Zn78, respectively, and indicate the presence of nearly spherical aggregates. The size dispersity indexes are 1.17 and 1.26 for Zn29 and Zn78, respectively, and are consistent with nearly monodisperse diameters. Both the mean aspect ratio and the size dispersity index were effectively constant as a function of annealing time.

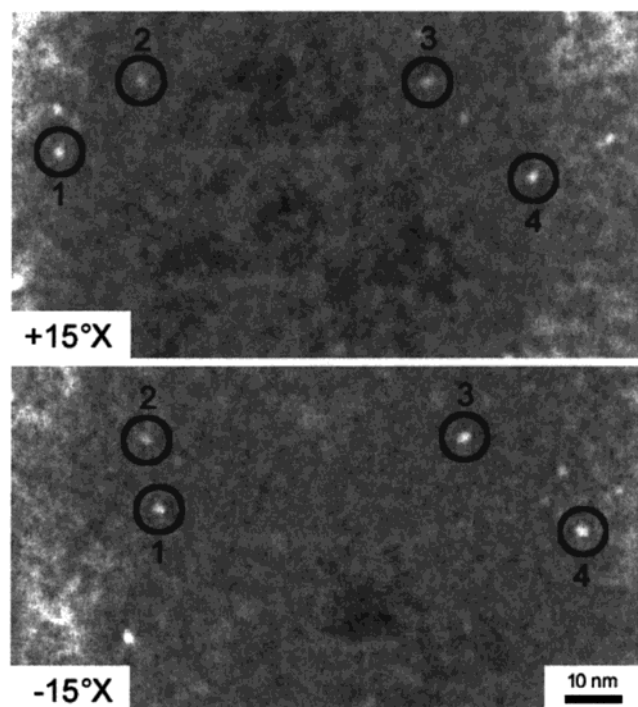


Figure 2. ADF-STEM tilt series of the as-extruded poly(ethylene-*ran*-methacrylic acid) random copolymer neutralized to 17% with Zn^{2+} . Angles correspond to the tilt angle about the y -axis. Table 1 contains the aspect ratio data for the individual aggregates identified (1–4) in the images.

Table 1. Aspect Ratios of the Individual Ionic Aggregates in Figure 2 as a Function of Tilt Angle about the y -Axis

aggregate	aspect ratios of aggregates		
	+15°	0°	–15°
1	1.13	1.02	1.13
2	1.13	1.14	1.20
3	1.14	1.08	1.17
4	1.00	1.25	1.11

The mean diameter of the Zn78 sample increases with annealing time, while the Zn29 sample does not increase significantly (Figure 5). We also found that the annealing conditions were sufficient for Zn29 pellets to flow into a single piece, while Zn78 pellets remained distinct pieces. This behavior is consistent with the viscosity of partially neutralized E/MAA ionomers increasing with neutralization level.¹⁰ Therefore, similar melt extrusion methods could trap Zn78 further from equilibrium. Consequently, during a quiescent anneal, the morphology of the more neutralized sample changes to a greater extent. Although the mean diameter of Zn78 increases from 1.70 to 2.81 nm, the difference between the final mean diameters of Zn29 and Zn78 is smaller than the uncertainty of the measurement. Thus, the mean diameter of the ionic aggregates remains independent of the neutralization level within the error of ± 1 pixel.

Images taken at lower magnifications illustrate the dramatic effect of recrystallization on the semicrystalline matrix of the ionomers. Parts a and b of Figure 6 are low and intermediate magnifications of the as-extruded Zn78 sample, while parts c and d of Figure 6 correspond to a recrystallized Zn78 sample. Though the ionic aggregates are not evident at the low magnification, the lamellar structure is much more pronounced in the recrystallized material. Similarly, at the intermediate magnification the crystalline lamellae of the matrix are better defined and larger in the recrystallized

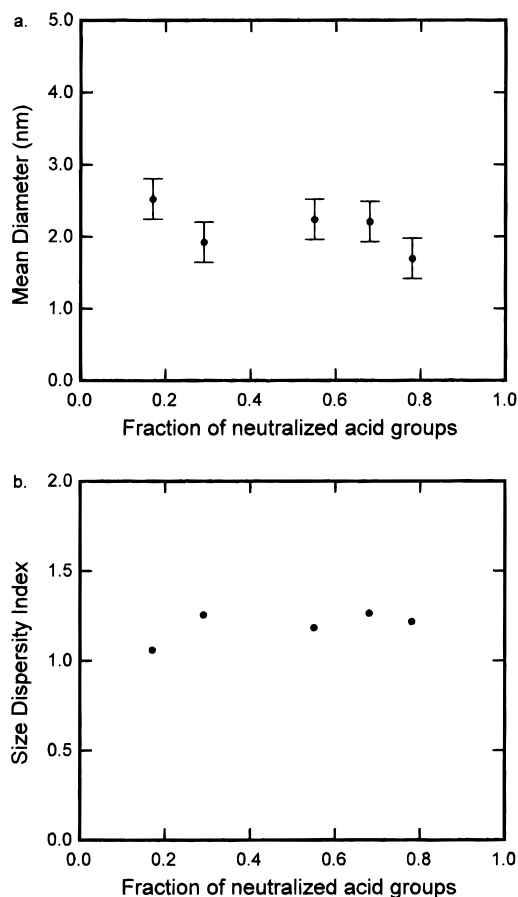


Figure 3. Mean diameter and size dispersity index for the as-extruded poly(ethylene-*ran*-methacrylic acid) random copolymer as a function of neutralization with Zn^{2+} . Error bars in mean diameter correspond to 1 pixel, 0.28 nm, at typical imaging conditions.

material. The ionic aggregates are also detected at the intermediate magnification at which the pixel size is 2.25 nm. Quiram et al. have shown in an E/MAA ionomer partially neutralized with Na that the “crystalline peak” moves to smaller angles upon recrystallization.² This observation was interpreted as an increase in the interlamellar spacing, which is consistent with our images.

Discussion

The ADF-STEM images present strong evidence that the ionic aggregates in partially Zn-neutralized E/MAA ionomers are spherical. Currently, the strongest evidence for spherical aggregate is the tilt series on the Zn17 specimen in which the feature shape and size are not complicated by overlap. Spherical ionic aggregates were found at all levels of neutralization (17–78%) and in both the as-extruded and recrystallized materials. While most scattering models have included spherical ionic aggregates, there is a notable exception. An interpretation of recent EXAFS data from partially Zn-neutralized E/MAA ionomers concludes that the aggregates are disklike such that the Zn atoms are coplanar.⁶ This interpretation further concludes that the aggregate size (disk diameter) increases with neutralization level. Our conviction is that the model-independent evidence from ADF-STEM images is more reliable in determining the shape of ionic aggregates. However, preliminary STEM results in our laboratory indicate that other ionomer systems exhibit nonspherical ionic aggregates.⁷

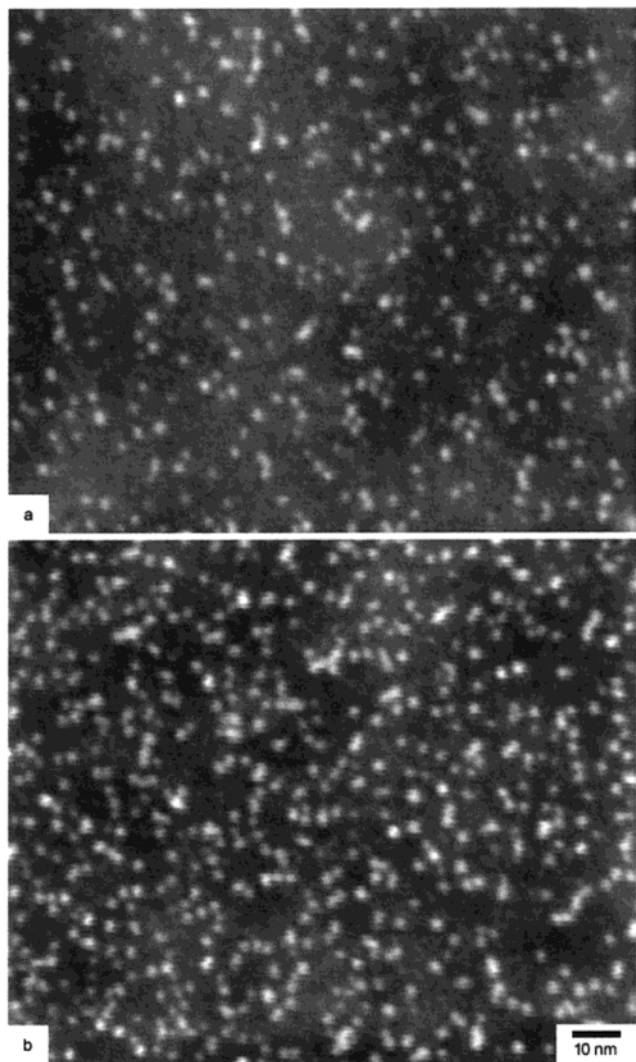


Figure 4. ADF-STEM images of poly(ethylene-*ran*-methacrylic acid) random copolymer neutralized to (a) 29% and (b) 78% with Zn^{2+} after annealing at 115 °C for 72 h and slowly cooling.

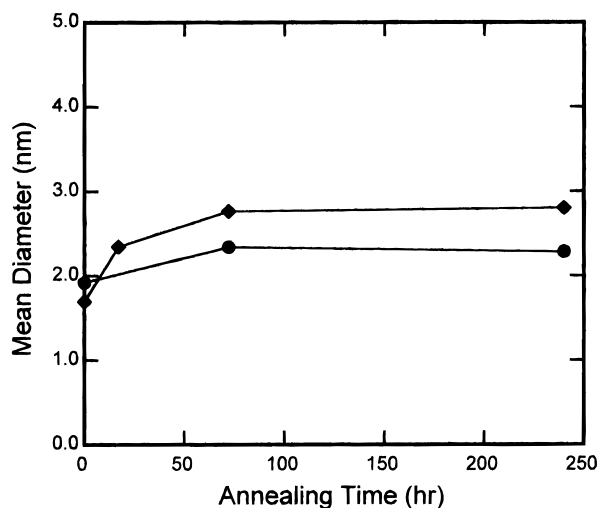


Figure 5. Mean diameter for the recrystallized poly(ethylene-*ran*-methacrylic acid) random copolymer neutralized to 29% (circles) and 78% (diamonds) with Zn^{2+} as a function of annealing time. Error bars in the mean diameter of 1 pixel, 0.28 nm, have been omitted from the plot for clarity.

The diameters of the ionic aggregates were measured to within 1 pixel, which is 0.28 nm with current imaging

conditions. Note that the absorption of water on the edge of the ionic aggregates⁶ does not alter the measured diameter of the Zn-rich aggregate because the scattering cross section is proportional to $\sim Z^2$. Furthermore, the presence of water is limited because the ~ 50 nm specimens are imaged at 10^{-6} Torr in the electron microscope. The observed diameters, ~ 2.1 nm, and size dispersity indexes, ~ 1.2 , of the ionic aggregates are independent of the extent of neutralization.

The Eisenberg–Hird–Moore model proposes spherical, monodisperse multiplets distributed nonuniformly in the matrix.¹¹ Regions of higher multiplet concentration are designated as clusters, and this multiplet-cluster morphology is used to describe the chain dynamics in ionomers. The EHM model argues that the multiplets exclude the polymer backbone due to the large difference in the electronegativity of the ionic species and the backbone. Here we will follow a method proposed by Eisenberg and Kim to determine the size of the ionic group and subsequently the number of cations in the multiplet.¹² A previous application of this analysis on poly(styrene-*co*-sodium methacrylate) ionomers determined that there are on the order of five cations per multiplet.¹³

Zinc acetate is used to model the ionic triplets in this study, because the EXAFS spectra of partially Zn-neutralized E/MAA ionomers is most consistent with this structure.⁵ Using the density, molecular formula, and molar mass of zinc acetate, the average volume per atom is 0.011 nm³. Within the ionomer each Zn^{2+} cation is associated with two methacrylic acid groups, such that the volume of this ionic triplet, which contains seven atoms, is ~ 0.077 nm³. The Zn-rich spherical aggregates observed in this study by ADF-STEM have a volume of 4.8 nm³ ($4\pi(1.05 \text{ nm})^3/3$). Consequently, if these aggregates are accurately described as multiplets, the aggregation number is ~ 65 cations per aggregate. Now consider the packing of ionic triplets, which are ~ 0.5 nm across, into an ionic aggregate that is ~ 2.1 nm in diameter. How do the ionic triplets reach the center of aggregate without pulling adjacent polymer backbone segments into the aggregate? Thus, the composition of the ionic aggregates is inconsistent with the description of multiplets in the EHM model.

Furthermore, it is unlikely that the observed aggregates correspond to the clusters in the EHM model. The EHM model correlates the second (higher) glass transition temperature with the matrix polymer chains within the clusters, because these chain segments have reduced mobility due to the multiplets. However, the uniformity of the intensity within the observed aggregates and the uniformity of the size and shape of the aggregates implies that these features are inconsistent with clusters. Thus, we continue to use the term “aggregates” in reference to the Zn-rich entities directly observed by STEM. In conclusion, the compositions of the ionic aggregates and the matrix need to be quantitatively measured to build upon this study which has determined shape, size, and size distribution of the aggregates. Such experiments are currently underway.

At present our discussion of the spatial distribution and the volume fraction of the ionic aggregates is qualitative, because we only nominally know our section thicknesses, ~ 50 nm. The ionic aggregates appear to be randomly distributed in the projected STEM images. This is consistent with the three-phase model in which

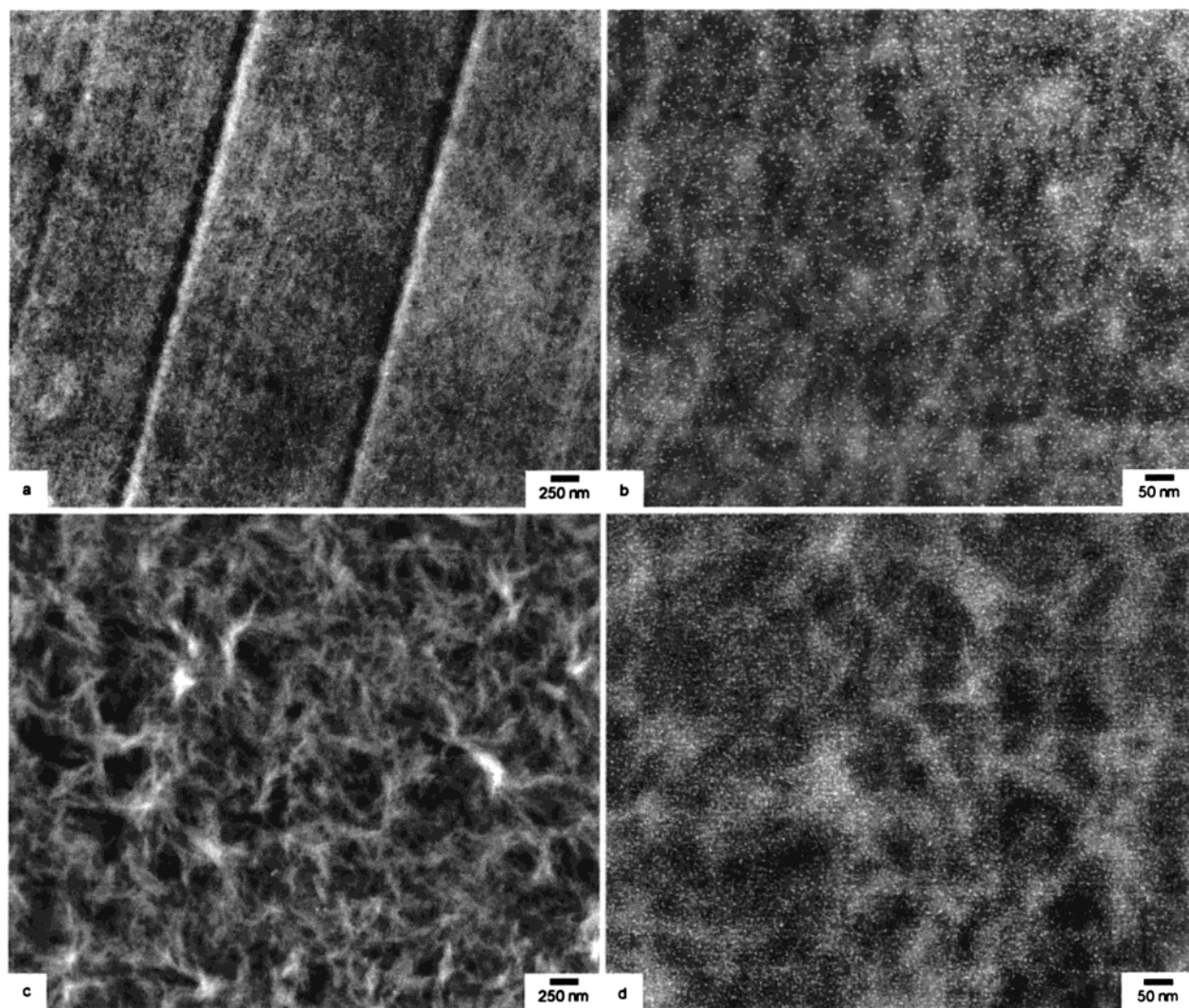


Figure 6. Lower magnification ADF-STEM images of poly(ethylene-*ran*-methacrylic acid) random copolymer neutralized to 78% with Zn^{2+} : (a, b) as-extruded; (c, d) recrystallized by annealing at 115 °C for 72 h and slowly cooling. Lamellar structure of semicrystalline matrix is more pronounced in the recrystallized material.

the aggregates reside between ~ 5 nm thick lamellae.⁵ However, the areal fraction of ionic aggregates changes dramatically between 17% and 29% neutralization. In fact, Figure 1a and Figure 2 of Zn17 exhibit areas as large as ~ 50 nm \times 50 nm void of ionic aggregates, unlike the more highly neutralized materials. Consequently, the ionic aggregates in Zn17 can be separated by more than the radius of gyration of the copolymer. Perhaps the fraction of cations contained in aggregates, that is the aggregation efficiency, dramatically increases between 17% and 29% neutralization, though compositional analysis of the matrix is needed to study this further.

Finally, we consider what controls the shape and size of the ionic aggregates in partially Zn-neutralized E/MAA ionomers. From the STEM images we know that (1) the aggregate shape and size are apparently independent of the extent of neutralization, (2) the distribution of aggregate size is narrow, and (3) the separation between aggregates can be larger than the polymer dimensions. We interpret these findings to indicate that neutralization is not uniform on each chain and that ionic triplets can dissociate and assemble in partially neutralized systems. Thus, we conclude that the aggregate size is primarily set by the nature of the ionic interactions of the system. The polymer chain is appar-

ently secondary with regard to setting the shape and size of the aggregates. A detailed analysis of the electrostatics associated with the ionic aggregates requires the assumption or knowledge of the aggregate composition, which is an issue discussed above. Further investigations are warranted to establish the relative importance of the electrostatic interactions and the polymer chain in establishing the shape and size of ionic aggregates in ionomers.

Conclusions

Model-independent analysis of the ionic aggregates in ionomers is possible by imaging with high-resolution scanning transmission electron microscopy. This study investigated a series of partially Zn-neutralized poly(ethylene-*ran*-methacrylic acid) ionomers to determine the shape, size, and size distribution of the Zn-rich ionic aggregates. Using tilt series and aspect ratios, the ionic aggregates were found to be spherical, independent of their thermal history and neutralization level. Typical imaging conditions measured the size of aggregates to within 1 pixel, 0.28 nm. To this level of accuracy the measured size dispersity index is consistent with nearly monodisperse aggregates, and the aggregate size is ~ 2.1 nm. Both were found to be independent of the neutral-

ization level. The model-independent aggregate size relative to the size of the ionic triplet ($\text{Zn}^{2+}(\text{COO}^-)_2$) suggests that the ionic aggregates include both ionic species and nonionic segments of the polymer backbone. Furthermore, our results suggest that the shape and size of ionic aggregates are primarily set by the electrostatic interactions of the system.

Acknowledgment. We thank Prof. B. Grady (University of Oklahoma), Dr. J. Paul (DuPont), and Prof. R. A. Register (Princeton University) for helpful discussions. We acknowledge Dr. R. E. Lakis for technical assistance with the JEOL 2010F. The work was supported by DuPont and the Petroleum Research Foundation. The analytical electron microscopy was funded by NSF-DMR 94-13550 and the Laboratory for the Research on the Structure of Matter.

References and Notes

- (1) Register, R. A.; Cooper, S. L. *Macromolecules* **1990**, *23*, 318.
 - (2) Quiram, D. J.; Register, R. A.; Ryan, A. J. *Macromolecules* **1998**, *31*, 1432.
 - (3) Verma, R.; Hsiao, B.; Biswas, A. *Polym. Prepr.* **1996**, *37*, 415.
 - (4) Longworth, R.; Vaughan, D. J. *Nature* **1968**, *218*, 85.
 - (5) Grady, B. P.; Floyd, J. A.; Genetti, W. B.; Vanhoorne, P.; Register, R. A. *Polymer* **1999**, *40*, 283.
 - (6) Welty, A.; Ooi, S.; Grady, B. P. *Macromolecules* **1999**, *32*, 2989.
 - (7) Kirkmeyer, B. P.; Weiss, R. A.; Winey, K. I. *Macromolecules*, manuscript in preparation.
 - (8) Laurer, J. H.; Winey, K. I. *Macromolecules* **1998**, *31*, 9106.
 - (9) Pennycook, S. J. *Annu. Rev. Mater. Sci.* **1992**, *22*, 171.
 - (10) Vanhoorne, P.; Register, R. A. *Macromolecules* **1996**, *29*, 598.
 - (11) Eisenberg, A.; Hird, B.; Moore, R. B. *Macromolecules* **1990**, *23*, 4098.
 - (12) Eisenberg, A.; Kim, J.-S. *Introduction to Ionomers*; John Wiley & Sons: New York, 1998.
 - (13) Eisenberg, A.; Bartels, C. *Macromol. Symp.* **1998**, *131*, 39.
- MA991374J